Available online at www.sciencedirect.com
SCIENCE DIRECT®
Neuroscience Research 45 (2003) 419–427
Neuroscience Research
www.elsevier.com/locate/neures

Sleep spindles in human prefrontal cortex: an electrocorticographic study

Motoaki Nakamura [a], Sunao Uchida [b,*], Taketoshi Maehara [c], Kensuke Kawai [c], Nobuhide Hirai [b], Tetsuo Nakabayashi [a], Hiroshi Arakaki [a], Yoshiro Okubo [a], Toru Nishikawa [a], Hiroyuki Shimizu [c]

[a] *Department of Psychiatry and Behavioral Science, Tokyo Medical and Dental University, Tokyo, Japan*
[b] *Department of Sleep Disorders Research, Tokyo Institute of Psychiatry, 2-1-8 Kamikitazawa, Setagaya-ku, Tokyo 156-8585, Japan*
[c] *Department of Neurosurgery, Tokyo Metropolitan Neurological Hospital, Tokyo, Japan*

Received 26 August 2002; accepted 24 December 2002

Abstract

To investigate the sleep spindle activity of the human prefrontal cortex (PFC), we simultaneously recorded whole nights of polysomnographic and electrocorticographic (ECoG) activities during the natural sleep of epileptic patients. Subjects were nine patients with intractable epilepsy who had subdural electrodes surgically attached to the orbital (seven cases), medial (three cases), or dorsolateral (two cases) PFC, and in one case to the frontal pole. To examine spindle frequencies, fast Fourier transformation (FFT) and auto-correlation analyses were performed on the PFC ECoG and Cz EEG data, primarily on epochs of stage 2 sleep. Lower sigma band ECoG oscillations of about 12 Hz were widely distributed across all prefrontal cortical areas including the frontal limbic regions, but none of the PFC sigma frequency peaks coincided with the faster (about 14 Hz) Cz EEG sleep spindles. Combining our results with anatomical and electrophysiological facts, it is suggested that the thalamofrontal circuit involving the rostral reticular and the mediodorsal nucleus of the thalamus is responsible for the generation of 12 Hz frontal spindles in humans.

Keywords: Human; Epileptic; Electrocorticogram; Sleep; Spindle oscillation; Prefrontal cortex; Mediodorsal nucleus of the thalamus; Reticular nucleus of the thalamus

1. Introduction

Neurophysiological studies have indicated that the EEG sleep spindle is a manifestation of thalamic inhibition produced during electrical synchronization within thalamocortical neuronal networks (Steriade and Llinas, 1988). Such spindle producing oscillation is considered to block afferent thalamic transmissions and thus functionally isolates the cortex from external stimuli (Steriade and Amzica, 1998). Thus, the maintenance and promotion of NREM sleep are considered to be functional roles reflected by the occurrence of sleep spindles.

In the human EEG, two types of sleep spindles have been described which differ in frequency and scalp distribution (Gibbs and Gibbs, 1950; Jankel and Niedermeyer, 1985); one with a frequency of about 14 Hz appears centro-parietally and the other, of about 12 Hz, appears in frontal regions. In EEG recordings from surface electrodes, frontal spindles tend to appear shortly after the first bursts of centro-parietal spindles with asymmetries observed frontally (Gibbs and Gibbs, 1950). Caderas et al. (1982) observed that frontal spindle activities in depth leads proceeded spindling on the scalp by minutes and appeared while the scalp EEG only showed patterns of light drowsiness. To date, 14 and 12 Hz spindles have been considered separately in only a few human sleep studies. To our knowledge, no animal study has yet distinguished among the heterogeneous mix of spindles with different frequencies and distributions.

* Corresponding author. Tel.: +81-3-3304-5701; fax: +81-3-3329-8035.
E-mail address: sunao@uchidae.com (S. Uchida).

0168-0102/03/$ - see front matter
doi:10.1016/S0168-0102(03)00007-5

Recently, there has been increased interest in human 12 Hz spindles. Werth et al. (1997) examined high and low frequency spindles separately and reported that the power of low frequency spindles showed a declining trend, while high frequency spindles showed a rising trend across consecutive NREM episodes. Shinomiya et al. (1999) analyzed central 14 Hz spindles and frontal 12 Hz spindles in children and adolescents, and found that the two types of spindle activity showed different maturational courses. The power of frontal spindles was greatest in young children (up to about 5 years old), and rapidly decreased across the first decade of life; by contrast, the spectral power of centro-parietal spindles changed little across age. A new technique of low-resolution electromagnetic tomography (LORETA) was recently applied in healthy subjects to investigate the relationships between spindle frequency and distribution (Anderer et al., 2001). LORETA demonstrated a source of low frequency spindles distributed in the prefrontal cortex (PFC) (Brodmann's areas 9 and 10), and high frequency spindles in the precuneus (Brodmann's area7). These differences between the two types of spindle strongly suggest there is heterogeneity in the spindle-producing properties of the underlying thalamocortical neuronal circuits.

We have had opportunities to record the natural sleep electrocorticogram (ECoG) from subdural electrodes implanted in patients with partial epilepsy. From their records, we have examined sleep spindles in various cortical regions, facing not only the calvaria but also the internal base of the skull and the longitudinal fissure. We have previously reported the absence of spindles in the cortical areas of the basal and medial temporal lobes (Nakabayashi et al., 2001). Here, we focus on the electrophysiological characteristics of sleep spindles in the most phylogenetically developed cortical structure in the human brain, the human PFC.

2. Materials and methods

2.1. Subjects

Subjects were nine patients with intractable epilepsy (seven males and two females, 20–47 years of age, average age 31.1 years) with subdural electrodes attached to the PFC at orbital (seven cases), medial (three cases) and dorsolateral (two cases) PFC and frontal pole (one case) areas. Electrodes were applied solely for the clinical purpose of evaluating the locations of epileptogenic foci, as indications for the neurosurgical treatment for partial seizures. In this group of patients it had been difficult to determine the primary foci using surface EEG and neuroimaging examinations, thus all patients required additional examinations through subdural electrode placements. No patients had undergone a lobectomy or a leukotomy prior to the sleep recordings, although one had undergone a prior callosotomy.

2.2. Procedures

During the neurosurgical operation, intracranial electrode sets were inserted into the subdural space through burr holes in the skull. One or more of three types of subdural electrode sets were attached to PFCs (see Fig. 1). A four electrode strip and a four electrode grid were used to record from the orbital and lateral surfaces of the PFC. A strip with four electrodes on each side was placed into the interhemispheric space to record signals from the right and left medial PFCs. For each electrode set, neighboring electrodes were separated by intervals of 10 mm. Subject profiles including the electrode type, position, and derivation, as well as the location of identified epileptogenic foci and prescribed anti-epileptic drugs (AEDs) are listed in Table 1.

To minimize the possible after-effects of the neurosurgical invasion and accompanying general anesthesia upon brain activities, all-night ECoG recordings were made approximately 1 week after the surgical placement of the subdural electrodes. Although several AEDs had been prescribed for all patients (Table 1), those drugs were discontinued for 3 days following electrode placement operation to remove the suppression of epileptic seizures and allow monitoring for clinical evaluation. Administration of AEDs resumed on the fourth day after the operation, and AEDs were, therefore, presumably influencing brain activities (Placidi et al., 2000; Sammaritano and Sherwin, 2000) during the all night sleep recordings.

In the present study, we did not systematically examine detailed differences in spindle activity between epileptogenic and non-epileptogenic hemispheres, but did exclude recordings from the successfully resected areas from the analyses. To minimize the possible influence of propagating epileptogenic discharges upon spindle bursts, epochs containing epileptogenic waveforms were carefully identified and excluded from the analyses.

On the day before sleep recording, each patient was conscious, alert, and could perform daily hospital activities independently. Each recording was performed the patient's hospital room beginning between 20:30 and 22:30 h and continuing for 8–10 h through the night.

In addition to ECoG, a scalp electroencephalogram (EEG) from Cz-A1 (placed according to the international 10–20 system), an oblique electro-oculogram (EOG) and a chin electromyogram (EMG) were recorded simultaneously to identify sleep stages. In three subjects, only bipolar recordings (BP) were made among subdural electrodes on the PFCs; in all others, monopolar recordings (MP) referenced to A1 (left mastoid) were performed (Table 1).

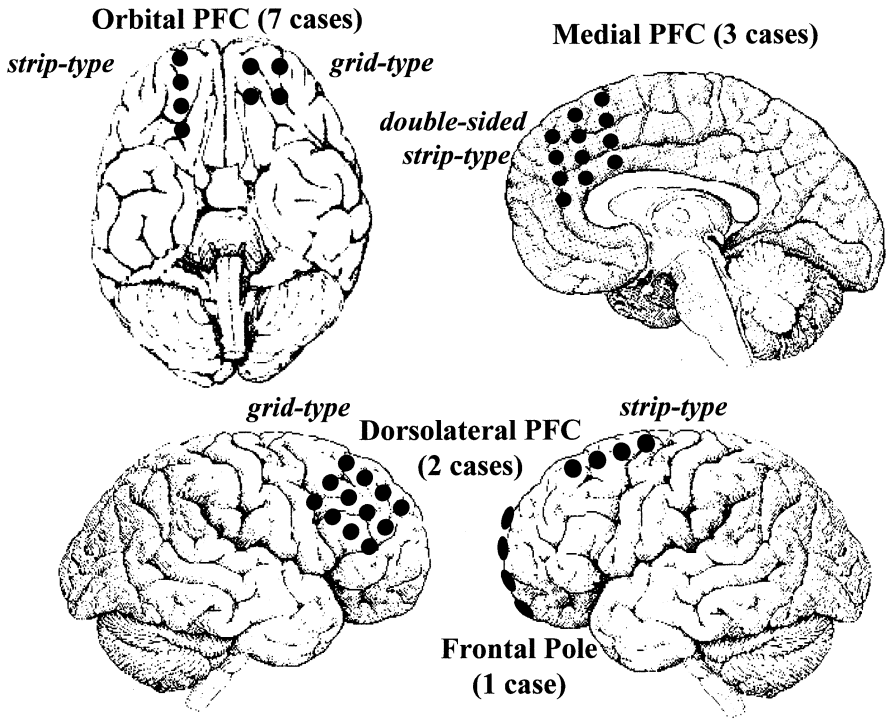

Fig. 1. Locations and types of subdural electrode arrays. Note that electrode positions exhibited in this schema approximate the individual placements on prefrontal cortices including orbital PFC, medial PFC, dorsolateral PFC and the frontal pole. Subdural electrode sets were a strip-type with either four electrodes on one edge or eight electrodes along two edges, and a grid-type on one side with either four or 12 electrodes, selected as suitable for each cerebral surface. Each electrode was spaced at regular intervals of 10 mm. Abbreviations: PFC, prefrontal cortex.

All signals were amplified and conditioned using a 32-channel bioamplifier ('Biotop' NEC Medical Systems, Tokyo), and recorded on either 28-channel FM analog data recorders ('XR-9000' TEAC Corporation, Tokyo) or a 32-channel digital data recorder ('SIR-1000' Sony Precision Technologies, Tokyo). No 50 Hz line filtering was performed. For ECoG and EEG recordings, a 0.5 Hz low cut filter and a 3000 Hz high cut filter were applied.

Data recorded on analog tape were digitized at 1500 Hz or above and decimated with a finite impulse response (FIR) high cut filter (cut-off frequency 300–350 Hz) to obtain 750 Hz digital data files, thus, frequencies from 0 to 375 Hz were available for analyses

Table 1
Subject Information

Case	Age/sex	Location of ICEs (strip, s; grid, g)	Derivation	Epileptogenic foci	Administered AEDs (mg/day)
1	25/F	lt. OFC (s)	MP/Al	bil. medial PFC (rt. > lt.)	CBZ 800
2	20/M	bil. OFC (g)	MP/Al	lt. lateral temporal lobe	VPA 1000, CBZ 500, ZNS 500
3	26/M	bil. OFC (g)	MP/Al	rt. medical temporal lobe	VPA 2000, PHT 375, PB 90, CZP 2.0, DZP 5.0
4	35/M	rt. DLPFC(g), rt. medial PFC(s), bil. frontal pole (s)	BP	rt. DLPFC	CBZ 600, PHT 300, CZP 1.5
5	32/F	bil. OFC (g)	BP	rt. medical temporal lobe	VPA 800, CBZ 1200, PHT 275, PB 120
6	34/M	lt. OFC (g)	MP/Al	rt. PFC (BA 8+6)	CBZ 800, PHT 150, PB 48
7	32/M	rt. OFC (s), rt. medial PFC (s), lt. Rolando's area (s)	BP	lt. PFC (BA 6)	VPA 1200, PB 120, ZNS 300
8	29/M	rt. OFC (g)	MP/Al	bil. medial temporal lobe	PHT 200, ZNS 300
9	47/M	rt. DLPFC (s), bil. medial PFC (s), corpus callosum (s)	MP/Al	lt. medial PFC (BA 9+10)	VPA 900, CBZ 900, DZP 11
Average	31.1 (20–47)				

Abbreviations: PFC, prefrontal cortex; OFC, orbitofrontal cortex; DLPFC, dorsolateral prefrontal cortex; ICE, intracranial electrode; MP/A1, monopolar derivation referenced to the electrode (A1) on the left mastoid; BP, bipolar derivation within the set of ICEs; BA, Brodmann's area; AED, anti-epileptic drug; CBZ, carbamazepine; VPA, sodium valproate; PHT, phenytoin; PB, phenobarbital; ZNS, zonisamide; CZP, clonazepam; DZP, diazepam.

after downloading onto a computer hard disk. Data recorded on digital tape were sampled at 1500 or 3000 Hz and decimated to 750 Hz using the same methods applied to analog data.

The Tokyo Institute of Psychiatry Ethics Committee approved the protocol of this study and written informed consent was obtained from each patient prior to recording.

2.3. Data analyses

Sleep stages were visually scored from a computer screen using standard criteria (Rechtschaffen and Kales, 1968) for each 16.4 s epoch (12 288 sampling points at 750 Hz sampling rate). Using the following criteria, 50 epochs were visually selected for fast Fourier transformation (FFT) spectral analysis from NREM sleep stages (mainly stage 2 sleep). Each analysis epoch included Cz EEG spindle waveforms, but did not necessarily include concurrent spindle waveforms in prefrontal ECoG, and was free from any recognizable artifacts. Spindle waveforms were visually identified using the criteria of a waxing and waning morphology and a length greater than 0.5 s (Rechtschaffen and Kales, 1968). The FFT analysis epoch length was 2048 points (ca. 2.7 s) beginning at the location of a visually placed cursor that located the starting point of the spindle epoch. Since one sequence of spindle bursts could last from 0.5 to 3 s, the 2048-point epoch length could include the greater part of most spindle sequences. A Hanning window was applied to each epoch prior to FFT analysis. The frequency resolution of the FFT was 0.366 Hz. For each electrode, the EEG and ECoG signal FFT power spectra obtained from the 50 epochs were averaged and the spectral power value peaks in the sigma frequency band were examined for each subject.

To assess across-night trends in the relationships between the sigma and delta frequency bands, all subjects' EEG and ECoG signals were FFT analyzed throughout each recording using consecutive 12 288-point (ca. 16.4 s) epochs, which were averaged as a sequence of six FFT-analyzed 2048-point sub-epochs. From this sequential FFT analysis, the temporal relationships between across night power fluctuations in the sigma and delta band activities of prefrontal ECoG and Cz EEG were compared.

For accurate measurement of each spindle's frequency, autocorrelation analysis was applied to 250-point (ca. 0.3 s) data from the spindle sequences in each subject's most spindle-abundant derivation. The peak correlation coefficient between 10.0 and 15.0 Hz was considered to identify spindle frequency. The distributions of intra-spindle frequencies were also compared between PFC ECoG and Cz EEG derivations in each case.

3. Results

In the visual observation of raw signals, spindle sequences were readily observed in the Cz EEG and all ECoG PFC derivations. The amplitude of the subdural PFC ECoG signals was typically about five times higher than that recorded from the scalp EEG at Cz (see Fig. 2). Many PFC spindles appeared to occur independent of EEG spindles at Cz.

To observe the temporal relationships between power measures of sigma and delta (0.3–3 Hz) band EEG and ECoG activity, consecutive FFTs were performed across each all-night recording. To specifically examine spindle activities, distinct sigma frequency bands were defined separately for the Cz EEG and the PFC ECoG of each case, using the spindle frequencies identified through the autocorrelation analysis described above. Fig. 3 presents representative across-night patterns of delta and sigma band power in the Cz EEG, and the left and right OFC ECoG with the corresponding sleep staged hypnogram from Case 2. In each NREM period the sigma power of Cz EEG increased initially, then decreased as delta power increased, as previously reported (Uchida et al., 1994, 1991). The same NREM sigma and delta activity relationships were also observed in the PFC ECoG. These trends were replicated in the other eight cases.

Fig. 4 presents the Cz EEG power spectra and simultaneously recorded PFC ECoG from the present nine cases. For these analyses, 50 epochs that included visually identified Cz EEG spindles were selected without regard for the existence or absence of ECoG spindles. All cases showed a clear Cz EEG sigma peak (mean 13.5 Hz), representing sleep spindle activities. In all but one case (Case 8) the PFC ECoG spectra also showed sigma peaks; however, all the unimodal PFC ECoG peaks were slower (mean 11.7 Hz) than the spindle frequency peak for the Cz EEG. Inter-subject and inter-electrode variations were obvious in the form, frequency and power values of sigma peaks. Spectral peaks in the sigma band were not observed from stage wake or stage REM. Although one case did not display an obvious PFC ECoG sigma peak, spindle sequences were visually observed, but the small amounts of spectral power were not reflected in the averaged sigma peak. In two cases, the Cz EEG sigma band contained bimodal peaks, with the less conspicuous slower peak sharing features with the PFC ECoG sigma peaks. The peak sigma activity from electrodes on the Rolandic area and in the trunk of the corpus callosum after callosotomy (Case 9) duplicated the sigma frequency peak in the Cz EEG.

Autocorrelation analysis was applied to the PFC ECoG and Cz EEG spindle waveforms. Spindle sequences in the PFC ECoG signals were found in all

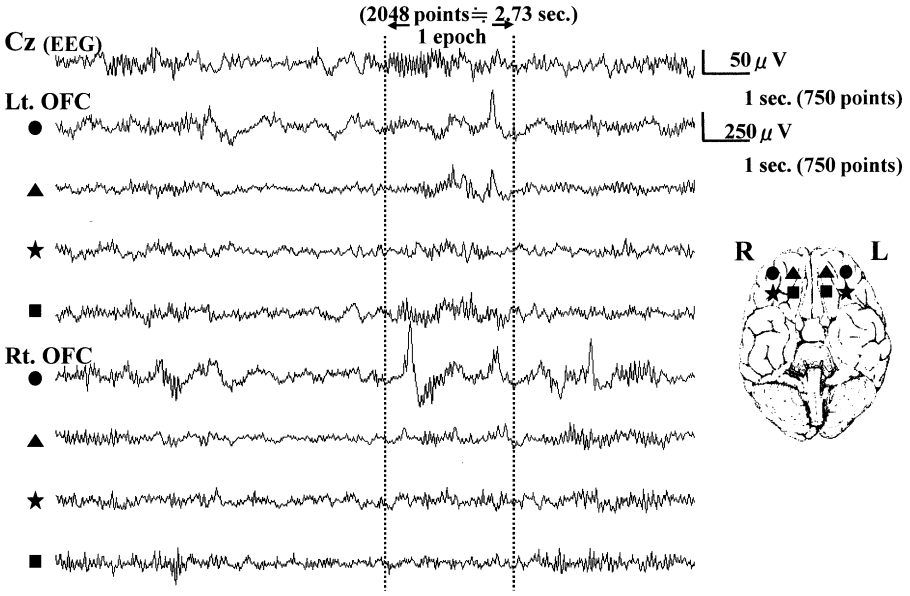

Fig. 2. Raw EEG and ECoG signals during NREM sleep in Case 2. A representative segment of raw signals from sleep stage 2 in Case 2. The top tracing indicates Cz EEG signals and the rest indicate OFC ECoG signals of about five times higher amplitude than EEG. All signals are monopolar, referenced to the left mastoid. The period between vertical dotted lines indicates one epoch of 2048 points length (2.73 s) for FFT analysis. In each epoch, a typical spindle sequence is observed in Cz EEG and in all derivations of OFC ECoG. These ECoG waveforms were not always synchronized bilaterally or with a Cz EEG spindle.

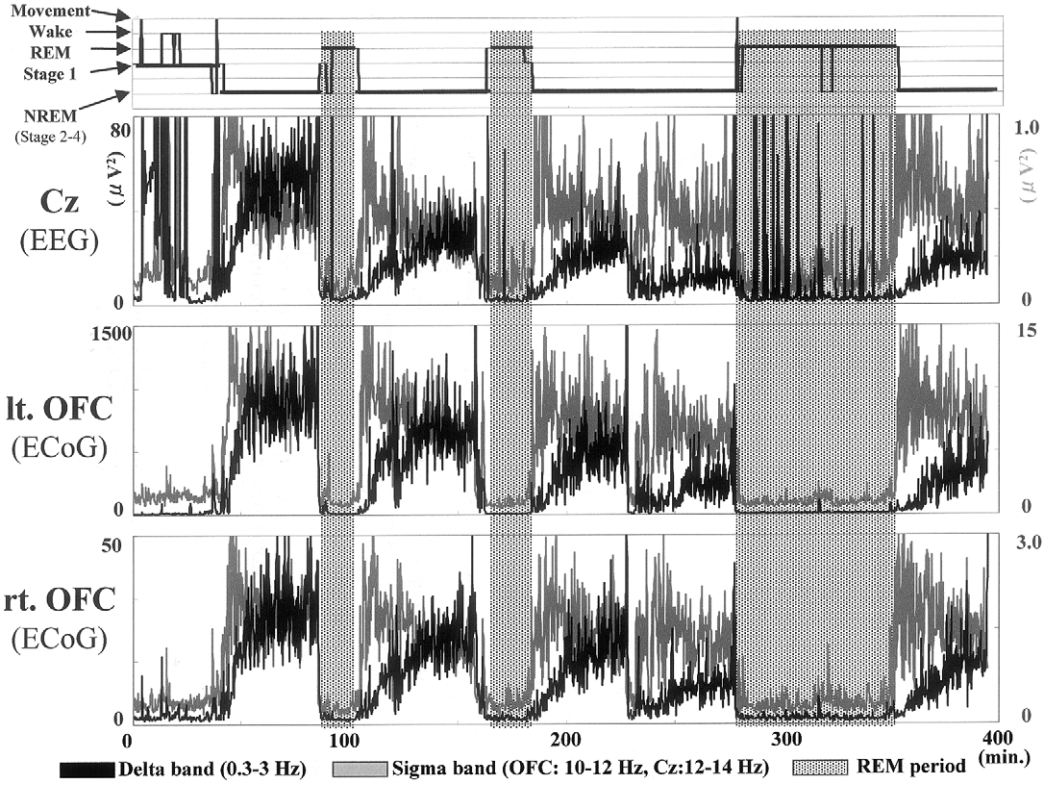

Fig. 3. Across-night power fluctuations of Cz EEG and bilateral OFC ECoG in Case 2, with hypnogram. Delta and sigma band activities are colored black and gray, respectively. The horizontal axis indicates time in minutes and vertical axes indicate power values with delta activity scaled on the left, and sigma activity on the right side, respectively. Sigma frequency bands are separately defined for Cz EEG (12–14 Hz) and PFC ECoG (10–12 Hz) in this case using the spindle frequencies obtained from autocorrelation analysis. The shaded portions indicate REM periods. During the NREM periods the power of Cz EEG sigma activities increases at first, and then delta power increases while sigma decreases. These inverse relationships between sigma and delta activities were also observed in OFC ECoG during NREM periods.

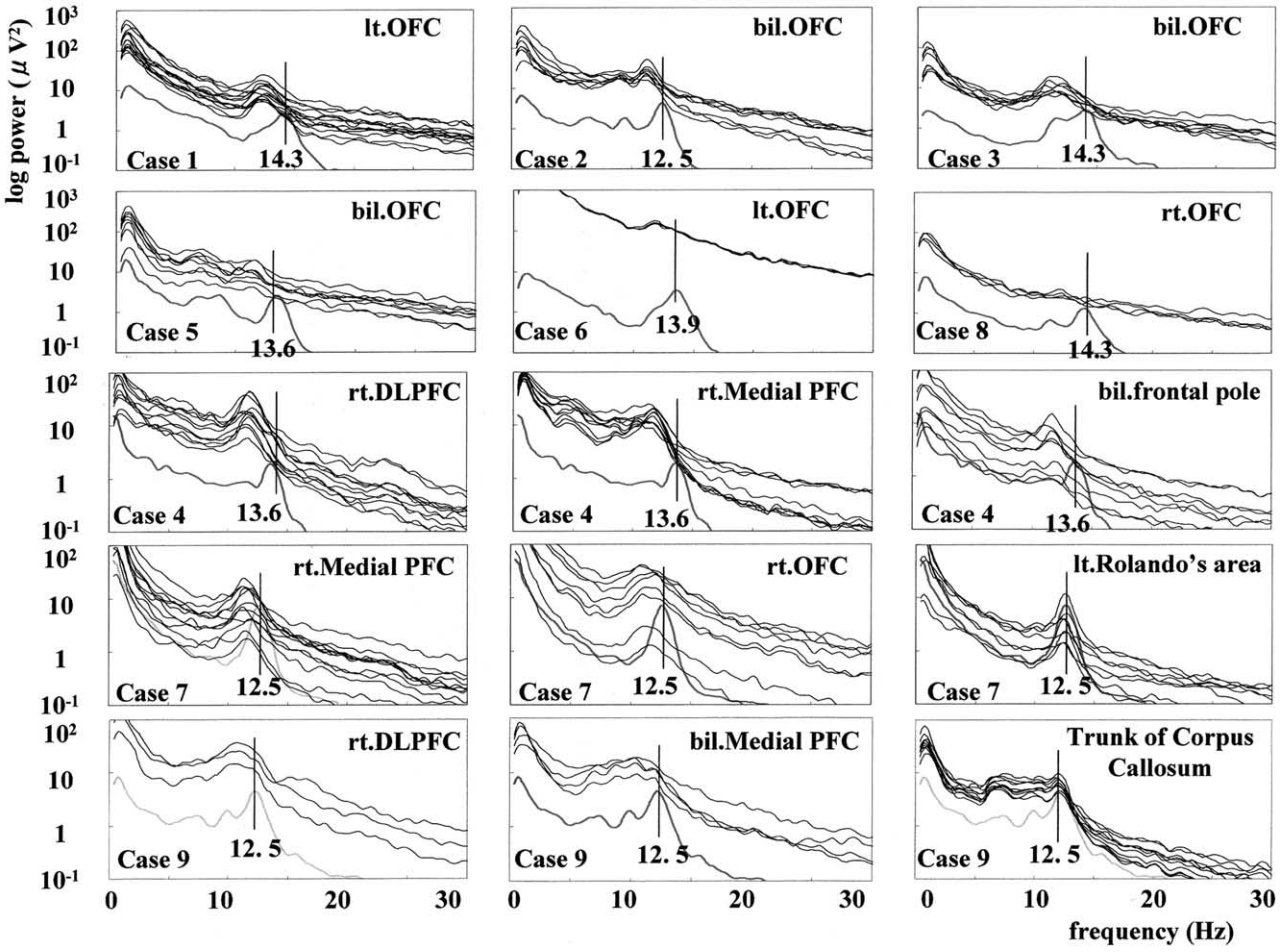

Fig. 4. Power spectra of prefrontal ECoG and Cz EEG in stage NREM. All nine cases' attached subdural electrodes from OFC, DLPFC, medial PFC, frontal pole and other cortical areas are shown in each graph. Fifty 2048-point (2.73 s) epochs were summed and averaged for each electrode. In each panel the thick gray line indicates the Cz EEG spectrum; other thin black lines with higher logarithmic power values indicate prefrontal ECoG spectra for each electrode. The sigma band Cz EEG frequency peaks, shown in Hertz (Hz), considered to represent the mean frequencies of sleep spindles are identified by vertical lines. All PFC ECoG spectra except for Case 8 exhibit prominent slower peaks in the sigma band than are seen in Cz EEG spectra. None of PFC ECoG spectra shows a consistent faster sigma peak than is seen for Cz EEG. In Cases 3 and 4, Cz exhibited bimodal sigma peaks, with the inconspicuous slower peak almost consistent with the PFC ECoG sigma peak. Inter-individual and inter-electrode variations in peak form, frequency and power values are evident in most cases. Note that Rolando's area for Case 7 and the trunk of the corpus callosum (i.e. white matter) for Case 9 show sigma peaks consistent with the Cz EEG spectrum. Abbreviations: PFC, prefrontal cortex; OFC, orbitofrontal cortex; DLPFC, dorsolateral prefrontal cortex.

cases, although the number of spindle epochs available for analysis varied among subjects. The average peak frequency in the sigma band was 11.7 ± 0.39 Hz ($n = 13$, range 11.1–12.4 Hz) in PFC ECoG, and 13.4 ± 0.72 Hz ($n = 9$, range 12.4–14.4 Hz) in Cz EEG. The difference between Cz EEG and PFC ECoG sigma peak frequencies was 1.7 ± 0.44 Hz ($n = 9$, range 1.0–2.2 Hz). The distributions of spindle frequencies obtained from the autocorrelation analysis are presented as a histogram in Fig. 5. In both the PFC ECoG and Cz EEG, it was evident that the spindle frequency derived from a given electrode fluctuated narrowly within a 1 Hz range throughout the night. Although six of nine cases showed narrowly overlapped PFC ECoG and Cz EEG spindle frequency ranges, all distributions were clearly divided into two distinct frequency bands.

4. Discussion

In the present study of intracranial ECoG, we demonstrated that low frequency spindle oscillations around 12 Hz were widely distributed across orbital, medial and dorsolateral PFCs and the frontal pole. With FFT and autocorrelation analyses, it was noted that none of the PFC ECoG spindle sigma frequency peaks occurred near the Cz EEG peak frequency of about 14 Hz. These differences between frontal and central spindle activities lead us to hypothesize that two distinct forms of spindle bursts propagate to the cortex through different and independent neuronal circuits.

Spindle oscillations are intermittent bursts of synchronized firing in thalamocortical neuronal circuits consisting of the reticular nucleus of the thalamus (RE),

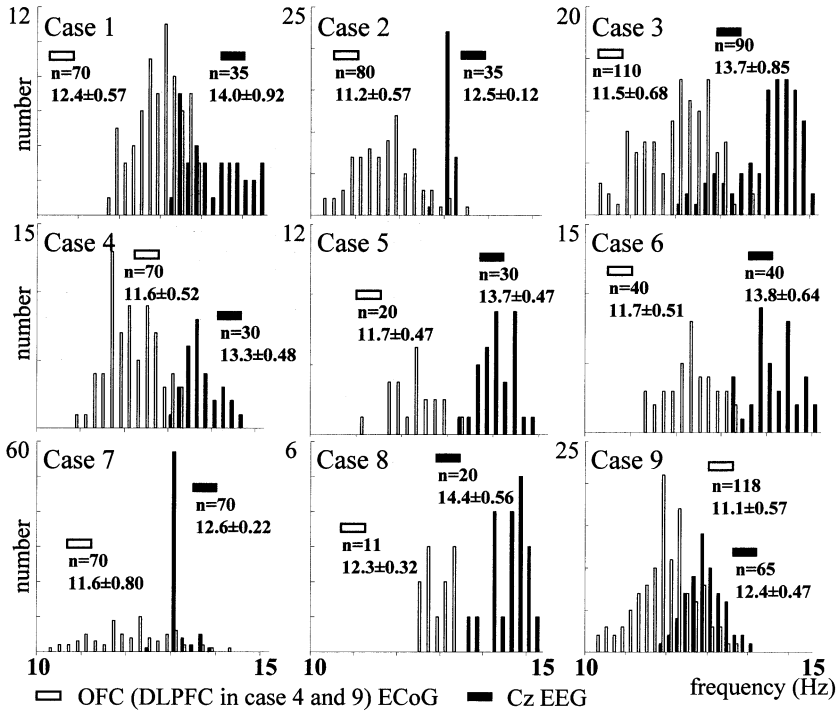

Fig. 5. Histograms of spindle frequencies obtained from autocorrelation analysis. White bars indicate spindle frequency distributions of PFC (OFC or DLPFC) ECoG and black bars indicate those of Cz EEG. In each histogram, the total number of 250-point-epochs analyzed is noted with the spindle frequency mean ± standard deviation (S.D.) in Hertz (Hz). For both ECoG and EEG, the spindle frequency derived from one electrode fluctuated within a 1 Hz range through the night. Except for Cases 1, 3, and 9, the ranges overlapped by PFC ECoG and Cz EEG spindle frequencies were narrow. In Cases 2 and 7, the frequency range of Cz EEG was clearly limited.

the thalamocortical neurons (TC) and the cortical pyramidal neurons (Cx) of layer 6 (McCormick and Bal, 1997; Steriade et al., 1993). It has been shown in animals that the thalamic reticular nucleus (RE) is the oscillator of sleep spindles, which result from its intrinsic membrane properties (Steriade et al., 1985, 1993). Spontaneous rhythmic bursts from the RE inhibit thalamocortical (TC) neurons synaptically through their divergent GABA-containing axons, resulting in a feed-forward inhibition of the neuronal network. The TC neurons are progressively hyperpolarized by RE neurons as they fire in the spindle frequency and the bursts of action potentials of the TC, in post-inhibitory rebound excitation, propagate to the pyramidal neurons of the cerebral cortex, resulting in the scalp-recorded sleep spindles (McCormick and Bal, 1997; Steriade et al., 1993).

The thalamus and the cerebral cortex are topographically linked by reciprocal projections. In primates, including humans, the prefrontal cortical regions—particularly the orbital, medial and dorsolateral PFCs—are known to receive afferent fibers from components of the mediodorsal nucleus of the thalamus (MD) (Fuster, 1997). It is also known that the MD receives fibers topographically from the rostral pole of the RE in the rat (Cornwall et al., 1990), cat (Steriade et al., 1984; Velayos et al., 1989) and monkey (Tai et al., 1995). Frontal limbic regions, including the anterior cingulate gyrus and orbitofrontal cortex (OFC), also receive afferent fibers from the anterior nucleus of the thalamus (AN) (Carmichael and Price, 1995). These GABAergic projections from the RE to the AN have been reported in the rat (Gonzalo-Ruiz and Lieberman, 1995; Lozsadi, 1995) and rhesus monkey (Kultas-Ilinsky et al., 1995). However, the AN of the cat does not receive fibers from the RE, and the AN does not display intracellular spindling oscillations (Mulle et al., 1985). Although details of human thalamoreticular pathways remain undefined, our results suggest the MD, rather than the AN, is more responsible for human frontal spindle activity. Since low frequency spindles were observed across a range of PFC areas in the present study, and since our previous study found a lack of spindle oscillations on human medial temporal cortical areas that receive afferent fibers from the AN (Nakabayashi et al., 2001), we speculate that the rostral RE–MD–PFC circuit is responsible for 12 Hz frontal spindles. Those slower PFC spindles manifested almost the same across-night pattern as the faster Cz EEG spindles (see Fig. 3), which also showed an inverse relationship with delta power within each NREM period (Aeschbach and Borbely, 1993; Uchida et al., 1994, 1991). The across-night coincidence of these PFC ECoG and Cz EEG sleep spindles suggests that the TC neurons

in the RE–MD–PFC circuit should also share the feature of spindle and delta incompatibility (Nunez et al., 1992).

It is possible that the present data from epileptic patients with intensive pharmacotherapy histories have limitations that might not reflect normal physiology. The effects of focal epileptic pathophysiology and AEDs upon spindle properties have been investigated in only a few reports. A slowing trend in intra-spindle frequency has been associated with idiopathic or secondary generalized seizures as well as phenobarbital administration and polypharmacy (Drake et al., 1991). An increasing trend in spindle density has been associated with the administration of GABAergic agents such as barbiturates and benzodiazepines (Hirshkowitz et al., 1982; Jobert et al., 1992; Johnson et al., 1976; Placidi et al., 2000; Sammaritano and Sherwin, 2000). By contrast, decreasing spindle density has been considered one characteristic of epileptic sleep (Sammaritano, 2001). However, it has also been reported that spindle intensity was slightly enhanced in the epileptogenic hemisphere compared with the unaffected hemisphere in most patients with partial epilepsy (Clemens and Menes, 2000). The location of an epileptic focus has also been related to changes in sleep stability and efficiency, with few effects seen in frontal lobe epilepsy, but fragmented sleep in temporal lobe epilepsy (Crespel et al., 2000). Our concern in this discussion is whether AEDs would have modified the topographic distributions of sleep spindles. The literature does not yet appear to have elucidated these relationships. However, it has been indicated that most AEDs bring about not disorganization but normalization and stabilization of patients' sleep either directly or indirectly (Sammaritano and Sherwin, 2000).

Although interpretations of the present ECoG study are limited due to the medicated epileptic population sampled, ECoG nevertheless demonstrated the significant advantage of recording field potentials directly—not only from cortices facing the calvaria, but also from other cortical areas facing the internal base of the skull and the longitudinal fissure. Moreover, the ECoG recordings reflected localized field potentials less influenced than surface EEG by outlying cortical area activities. Thus, within these human brains, analyses of ECoG enabled detailed observations of differing thalamocortical neuronal projections, as postulated above.

Our present results also suggest that it may be clinically worthwhile to investigate these two types of spindles separately since they seem likely to reflect different neuronal populations. For example, paramedian thalamic stroke (PTS) (Bassetti et al., 1996) and fatal familial insomnia (FFI) (Gallassi et al., 1996; Lugaresi et al., 1998) are both known to have relatively selective pathology within the MD. While the clinical manifestations are opposites, with hypersomnia presenting for PTS, and insomnia for FFI, both PTS and FFI manifest a reduction or deficit of sleep spindle activity, which could be related to MD neuronal dysfunction or rostral RE–MD–PFC neuronal circuit disruption. We would anticipate finding low frequency frontal spindles to be more specifically altered, although low and high frequency spindles have not yet been separately analyzed in these clinical studies. In Parkinsonian patients, medial thalamotomy has been shown to abolish spindle activity in NREM periods (Roth et al., 2000). Although no clinical disorder is known to uniquely affect it, the RE is known to be selectively vulnerable in severe head injury (Ross et al., 1993) or ischemic brain damage following cardiac arrest (Kawai et al., 1995; Ross and Graham, 1993). In such clinical cases, it may be worthwhile to further evaluate changes in spindle activity and clinical manifestations of RE damage.

Neuronal networks involving PFC and MD neurons have been studied in connection with cognitive and emotional aspects (Alexander et al., 1990; Cummings, 1993; Miller and Cummings, 1998). On the hypothesis that low frequency frontal spindles reflect specific activities within the rostral RE–MD–PFC circuit, alterations in frontal spindle oscillations of the surface EEG could be a biological marker indicating pathophysiological involvement of the thalamofrontal neuronal circuit. Thus, it may be possible to elucidate pathophysiology and maturation of the thalamofrontal circuit by examining frontal EEG properties such as the spindle frequency band, power intensity, density, or phase synchronicity. Such information could prove to correlate with cognitive dysfunctions or even psychotic symptoms.

Acknowledgements

We are grateful to Professor Irwin Feinberg of the University of California at Davis, Professor Hideshi Shibata of the Tokyo University of Agriculture and Technology, Dr Thomas Maloney of the State University of New York at Stony Brook and Dr Kuniaki Tanaka of Tokyo Medical and Dental University for critical readings of earlier versions of this manuscript.

References

Aeschbach, D., Borbely, A.A., 1993. All-night dynamics of the human sleep EEG. J. Sleep Res. 2, 70–81.

Alexander, G.E., Crutcher, M.D., DeLong, M.R., 1990. Basal ganglia–thalamocortical circuits: parallel substrates for motor, oculomotor, 'prefrontal' and 'limbic' functions. Prog. Brain Res. 85, 119–146.

Anderer, P., Klosch, G., Gruber, G., Trenker, E., Pascual-Marqui, R.D., Zeitlhofer, J., Barbanoj, M.J., Rappelsberger, P., Saletu, B., 2001. Low-resolution brain electromagnetic tomography revealed

simultaneously active frontal and parietal sleep spindle sources in the human cortex. Neuroscience 103, 581–592.
Bassetti, C., Mathis, J., Gugger, M., Lovblad, K.O., Hess, C.W., 1996. Hypersomnia following paramedian thalamic stroke: a report of 12 patients. Ann. Neurol. 39, 471–480.
Caderas, M., Niedermeyer, E., Uematsu, S., Long, D.M., Nastalski, J., 1982. Sleep spindles recorded from deep cerebral structures in man. Clin. Electroencephalogr. 13, 216–225.
Carmichael, S.T., Price, J.L., 1995. Limbic connections of the orbital and medial prefrontal cortex in macaque monkeys. J. Comp. Neurol. 363, 615–641.
Clemens, B., Menes, A., 2000. Sleep spindle asymmetry in epileptic patients. Clin. Neurophysiol. 111, 2155–2159.
Cornwall, J., Cooper, J.D., Phillipson, O.T., 1990. Projections to the rostral reticular thalamic nucleus in the rat. Exp. Brain Res. 80, 157–171.
Crespel, A., Coubes, P., Baldy-Moulinier, M., 2000. Sleep influence on seizures and epilepsy effects on sleep in partial frontal and temporal lobe epilepsies. Clin. Neurophysiol. 111 (Suppl 2), S54–S59.
Cummings, J.L., 1993. Frontal–subcortical circuits and human behavior. Arch. Neurol. 50, 873–880.
Drake, M.E., Jr, Pakalnis, A., Padamadan, H., Weate, S.M., Cannon, P.A., 1991. Sleep spindles in epilepsy. Clin. Electroencephalogr. 22, 144–149.
Fuster, J.M., 1997. The Prefrontal Cortex: Anatomy, Physiology, and Neuropsychology of the Frontal Lobe. Lippincott-Raven Publishers, Philadelphia, New York.
Gallassi, R., Morreale, A., Montagna, P., Cortelli, P., Avoni, P., Castellani, R., Gambetti, P., Lugaresi, E., 1996. Fatal familial insomnia: behavioral and cognitive features. Neurology 46, 935–939.
Gibbs, F.A., Gibbs, E.L., 1950. Atlas of Electroencephalography. Addison-Wesley Publishing Company Inc, Reading, MA, USA.
Gonzalo-Ruiz, A., Lieberman, A.R., 1995. Topographic organization of projections from the thalamic reticular nucleus to the anterior thalamic nuclei in the rat. Brain Res. Bull. 37, 17–35.
Hirshkowitz, M., Thornby, J.I., Karacan, I., 1982. Sleep spindles: pharmacological effects in humans. Sleep 5, 85–94.
Jankel, W.R., Niedermeyer, E., 1985. Sleep spindles. J. Clin. Neurophysiol. 2, 1–35.
Jobert, M., Poiseau, E., Jahnig, P., Schulz, H., Kubicki, S., 1992. Topographical analysis of sleep spindle activity. Neuropsychobiology 26, 210–217.
Johnson, L.C., Hanson, K., Bickford, R.G., 1976. Effect of flurazepam on sleep spindles and K-complexes. Electroencephalogr. Clin. Neurophysiol. 40, 67–77.
Kawai, K., Nowak, T.S., Jr, Klatzo, I., 1995. Loss of parvalbumin immunoreactivity defines selectively vulnerable thalamic reticular nucleus neurons following cardiac arrest in the rat. Acta Neuropathol. (Berl.) 89, 262–269.
Kultas-Ilinsky, K., Yi, H., Ilinsky, I.A., 1995. Nucleus reticularis thalami input to the anterior thalamic nuclei in the monkey: a light and electron microscopic study. Neurosci. Lett. 186, 25–28.
Lozsadi, D.A., 1995. Organization of connections between the thalamic reticular and the anterior thalamic nuclei in the rat. J. Comp. Neurol. 358, 233–246.
Lugaresi, E., Tobler, I., Gambetti, P., Montagna, P., 1998. The pathophysiology of fatal familial insomnia. Brain Pathol. 8, 521–526.
McCormick, D.A., Bal, T., 1997. Sleep and arousal: thalamocortical mechanisms. Annu. Rev. Neurosci. 20, 185–215.
Miller, B.L., Cummings, J.L., 1998. In: Bronstein, R.A. (Ed.), The Human Frontal Lobes: Functions and Disorders. The Guilford Press, New York, London.
Mulle, C., Steriade, M., Deschenes, M., 1985. Absence of spindle oscillations in the cat anterior thalamic nuclei. Brain Res. 334, 169–171.
Nakabayashi, T., Uchida, S., Maehara, T., Hirai, N., Nakamura, M., Arakaki, H., Shimizu, H., Okubo, Y., 2001. Absence of sleep spindles in human medial and basal temporal lobes. Psychiatry Clin. Neurosci. 55, 57–65.
Nunez, A., Curro Dossi, R., Contreras, D., Steriade, M., 1992. Intracellular evidence for incompatibility between spindle and delta oscillations in thalamocortical neurons of cat. Neuroscience 48, 75–85.
Placidi, F., Scalise, A., Marciani, M.G., Romigi, A., Diomedi, M., Gigli, G.L., 2000. Effect of antiepileptic drugs on sleep. Clin. Neurophysiol. 111 (Suppl 2), S115–S119.
Rechtschaffen, A., Kales, A., 1968. A manual of standardized terminology, techniques and scoring system for sleep stages of human subjects. Public Health Service, Washington, DC, Government printing office.
Ross, D.T., Graham, D.I., 1993. Selective loss and selective sparing of neurons in the thalamic reticular nucleus following human cardiac arrest. J. Cereb. Blood Flow Metab. 13, 558–567.
Ross, D.T., Graham, D.I., Adams, J.H., 1993. Selective loss of neurons from the thalamic reticular nucleus following severe human head injury. J. Neurotrauma 10, 151–165.
Roth, C., Jeanmonod, D., Magnin, M., Morel, A., Achermann, P., 2000. Effects of medial thalamotomy and pallido-thalamic tractotomy on sleep and waking EEG in pain and Parkinsonian patients. Clin. Neurophysiol. 111, 1266–1275.
Sammaritano, M., 2001. Focal Epilepsy and Sleep. In: Dinner, D, Lüders, H. (Eds.), Epilepsy and Sleep: Physiological and Clinical Relationships. Academic press, San Diego, California. pp. 85–100.
Sammaritano, M., Sherwin, A., 2000. Effect of anticonvulsants on sleep. Neurology 54, S16–S24.
Shinomiya, S., Nagata, K., Takahashi, K., Masumura, T., 1999. Development of sleep spindles in young children and adolescents. Clin. Electroencephalogr. 30, 39–43.
Steriade, M., Amzica, F., 1998. Coalescence of sleep rhythms and their chronology in corticothalamic networks. Sleep Res. Online 1, 1–10.
Steriade, M., Llinas, R.R., 1988. The functional states of the thalamus and the associated neuronal interplay. Physiol. Rev. 68, 649–742.
Steriade, M., Parent, A., Hada, J., 1984. Thalamic projections of nucleus reticularis thalami of cat: a study using retrograde transport of horseradish peroxidase and fluorescent tracers. J. Comp. Neurol. 229, 531–547.
Steriade, M., Deschenes, M., Domich, L., Mulle, C., 1985. Abolition of spindle oscillations in thalamic neurons disconnected from nucleus reticularis thalami. J. Neurophysiol. 54, 1473–1497.
Steriade, M., McCormick, D.A., Sejnowski, T.J., 1993. Thalamocortical oscillations in the sleeping and aroused brain. Science 262, 679–685.
Tai, Y., Yi, H., Ilinsky, I.A., Kultas-Ilinsky, K., 1995. Nucleus reticularis thalami connections with the mediodorsal thalamic nucleus: a light and electron microscopic study in the monkey. Brain Res. Bull. 38, 475–488.
Uchida, S., Maloney, T., March, J.D., Azari, R., Feinberg, I., 1991. Sigma (12–15 Hz) and delta (0.3–3 Hz) EEG oscillate reciprocally within NREM sleep. Brain Res. Bull. 27, 93–96.
Uchida, S., Atsumi, Y., Kojima, T., 1994. Dynamic relationships between sleep spindles and delta waves during a NREM period. Brain Res. Bull. 33, 351–355.
Velayos, J.L., Jimenez-Castellanos, J., Jr, Reinoso-Suarez, F., 1989. Topographical organization of the projections from the reticular thalamic nucleus to the intralaminar and medial thalamic nuclei in the cat. J. Comp. Neurol. 279, 457–469.
Werth, E., Achermann, P., Dijk, D.J., orbely, A.A., 1997. Spindle frequency activity in the sleep EEG: individual differences and topographic distribution. Electroencephalogr. Clin. Neurophysiol. 103, 535–542.